JOURNAL OF MATERIALS SCIENCE 12 (1977) 1750–1758

The initial stages of growth and the origin of proximate voids in boron fibres

JORGE VEGA-BOGGIO, OLOF VINGSBO
University of Uppsala, Institute of Technology, Uppsala, Sweden

JAN-OTTO CARLSSON
University of Uppsala, Institute of Chemistry, Department of Inorganic chemistry, Uppsala, Sweden

The formation of so-called proximate voids (i.e. voids near the core–mantle interface) in boron fibres has been studied experimentally. The mantle growth was interrupted in very early stages of nucleation and growth of boron nodules on the tungsten wire substrate. Scanning electron microscope investigations of surface topography and cross-sections revealed a morphology of preferential nucleation of boron nodules along axial die-mark ridges on the tungsten wire surface, where tight parallel axial rows of growing nodules are formed which, particularly around deep wire surface grooves, may hedge in axially extended voids of a morphology earlier found to be typical of proximate voids. The physical conditions of this mechanism are studied with respect to geometry, surface energy and diffusion parameters.

1. Introduction

The fracture of boron and so-called boron fibres is experimentally found to be brittle, even at very high temperatures. The origin of failure in the fibres can often be traced to a void or pore existing in the boron mantle in the immediate vicinity of the core–mantle interface [1–4]. These voids are referred to as "proximate voids". Wawner [1] attributed the formation to rapid diffusion of boron into the tungsten substrate, and subsequent vacancy condensation along the core–mantle interface. Layden [2] proposed the formation of voids in terms of a slower deposition rate of boron at the bottom of a substrate notch, leading to the occlusion of a void. The diffusion induced mechanism, suggested by Wawner, received some support by Vega and Vingsbo [3]. They measured the void–core diffusion distances and, by applying Einstein's formula for self-diffusion, obtained values of the self-diffusion activation energy (E_D) for boron between 1.9 and 2.2 eV. In a more recent work, Vega and Vingsbo [4] studied the morphology of proximate voids. They found transverse dimensions of the order of some microns, but often considerably longer axial extensions. They also observed irregularities, some of which could act as stress raisers and initiate transverse fracture under tensile testing, in agreement with the Griffith criterion for brittle fracture [5].

As far as the authors know, no complete explanation of the origin of proximate voids in boron fibres has yet been given. The fact that the proximate voids have been observed exclusively in the neighbourhood of the core–mantle interface, suggests that the formation is connected to the beginning of the deposition process. Therefore, the present studies were concentrated on the initial stages of growth.

2. Material and experimental

2.1. Production of fibres

A 16 cm length of tungsten wire, with diameter 14 μm, was placed in a horizontal deposition chamber with volume of 1.3 litres. The wire was resistively heated to 1100° C with direct current in hydrogen (6.7×10^4 Pa) for five minutes, in order to reduce tungsten oxides on the wire surface.

After reduction, the deposition chamber was evacuated and flushed several times with hydrogen. A reaction mixture, containing hydrogen and boron trichloride in a mole ratio of 5:1, was then introduced to a pressure of 6.7×10^4 Pa, and the deposition chamber was closed. The temperature of the wire was raised to about 1100° C in less than 1 sec, and kept at this temperature for about 2 sec. The fibre was produced under natural convection of the reaction gas mixture. Because of the short reaction time, the same results could have been obtained in a forced convective system of the type used in production of continuous fibres.

The variation of the resistivity of tungsten with temperature, together with optical micropyrometry were used to estimate the temperature. The pyrometer was preset to a desired temperature and during the fibre production the substrate temperature was matched to the temperature of the pyrometer filament. This method has a good reproducibility and the accuracy of the temperature measurements was estimated to ± 50°.

However, with the reaction gas composition used, the desired cap-shaped boron embryos were obtained within a rather wide temperature range (1000 to 1400° C) in less than two seconds. Thus, the reaction temperature is not a critical parameter, and the estimated uncertainty in temperature measurement is well tolerable. A detailed description of the deposition equipment will be given elsewhere [6].

2.2. Specimen preparation and electron microscopy

Tungsten wires of the type used as substrates, as well as fibres produced according to 2.1., were cut into pieces of 10 mm length.

Specimens for observation of the cylindrical surfaces were mounted in holders, washed, given a 300 Å thick gold coating by sputtering and observed in emissive mode with a JEOL JSM-U3 scanning electron microscope, operated at 20 kV.

Specimens for observation of cross-sections were given an electrolytical coating of nickel, according to a method described earlier by Hogmark *et al.* [7]. The resulting composites were mounted in epoxy resin and cut in 0.5 mm thick slices by means of a low-speed diamond saw. One of the sides of the slices was subsequently polished with 3 μm, 1 μm and 0.25 μm diamond spray on petrodiscs. The opposite sides were ground on a 45 μm diamond grinding disc, down to a total specimen thickness of 100 μm. (Thicker specimens resulted in SEM images of high astigmatism, undoubtedly due to the nickel coating.) Final mechanical polishing with diamond spray resulted in cracks and core–mantle decohesion failure, making high resolution observation both difficult and irrelevant. A far better result was obtained when the specimens were further polished by means of an argon-ion beam. Suitable polishing conditions were found to be an accelerating voltage of 8 kV, a current density of 11 to 14 A m^{-2} and a glancing angle of 10°. The specimens were subsequently coated with a 200 Å thick gold film and observed in emissive mode with a JEOL JEM-200 B scanning transmission electron microscope operated at 200 kV.

3. Results and discussion

3.1. The substrate

A SEM micrograph of a normal cross-section of a tungsten wire before deposition is reproduced in Fig. 1. It can be seen that the wire is not perfectly round and that its surface is not smooth. Fig. 2 shows that the surface irregularities are made up of die-marks from the drawing process, in the form of axial grooves and ridges.

3.2. The initial stages of fibre growth

3.2.1. Nucleation

In an earlier investigation, Wawner [1] emphasized the importance of the substrate surface for the nucleation of boron nodules. He even suggested that the ordered appearance of the surface of the final boron fibres could be attributed to die-marks on the substrate. Wawner showed that, when

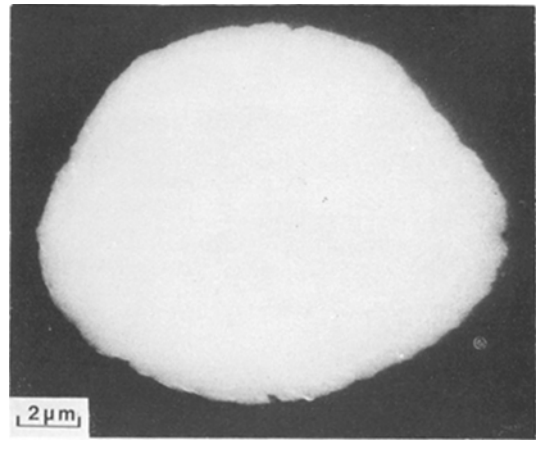

Figure 1 Polished normal cross-section of a tungsten wire. The nominal diameter of the wire is 14 μm. (200 kV SEM)

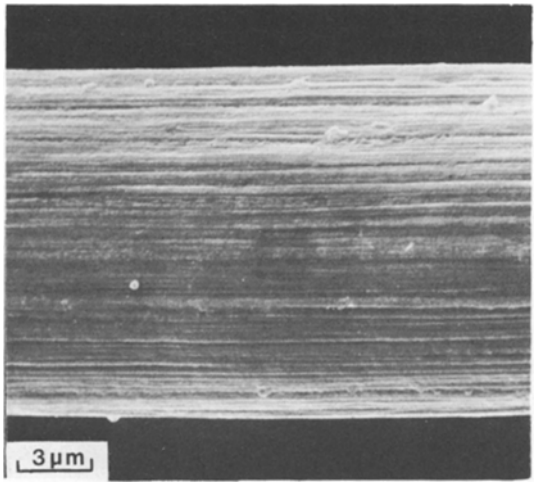

Figure 2 The prismatic surface of the wire of Fig. 1. (20 kV SEM)

depositing boron on a scratched tungsten sheet, preferential nucleation and initial growth could be observed "adjacent to the scratches". Careful observation of Wawners light optical micrographs shows, however, that the image resolution does not allow a precise localization of the nucleation sites relative to the scratches.

In the present investigation, therefore, the influence of substrate surface imperfections during the initial stages of growth of boron fibres, was studied with the aid of high resolution SEM as described in 2.2.

Figs 3a and b show cross-sections of a tungsten fibre, immediately after nucleation of the first boron nodules. The two micrographs represent consecutive transverse planes, separated in the axial direction (by repeated ion etching) by less than 0.2 µm, i.e. considerably less than one nodule diameter. It is obvious that boron nodule nucleation takes place preferentially at the die-mark ridges.

Fig. 4 shows the nodules at A and B of Fig. 3 in higher magnification. In this image, the specimen is tilted by 45° with respect to the imaging electron beam, whereby a topographic contrast, superimposed on the atomic number contrast of Fig. 3, reveals the topography after etching. It can be seen that the wetting and penetration of the embedding nickel is excellent, and that boron is preferentially attacked by the ion etching with respect to tungsten and nickel.

Fig. 5 is a SEM micrograph of the mantle surface during nucleation of the first boron nodules. The image clearly proves that they are nucleated in axial rows, the distance between successive nodules along a row being shorter than the distance between neighbouring rows.

The combined interpretation of Figs 3 and 5 immediately suggests a morphology of essentially tight rows of boron nodules, nucleated on die-mark ridges. This is an essential feature for the subsequent growth of the boron mantle. The phenomenon may be interpreted in terms of two competing mechanisms, one being based on boron diffusion, the other on surface energy considerations as follows:

(i) A boron layer of a constant, rather low surface concentration is formed extremely rapidly at the start of the process under the present experimental conditions (see Fig. 6a). Boron is added to the layer by deposition at a rate, which may be assumed constant during the short reaction time

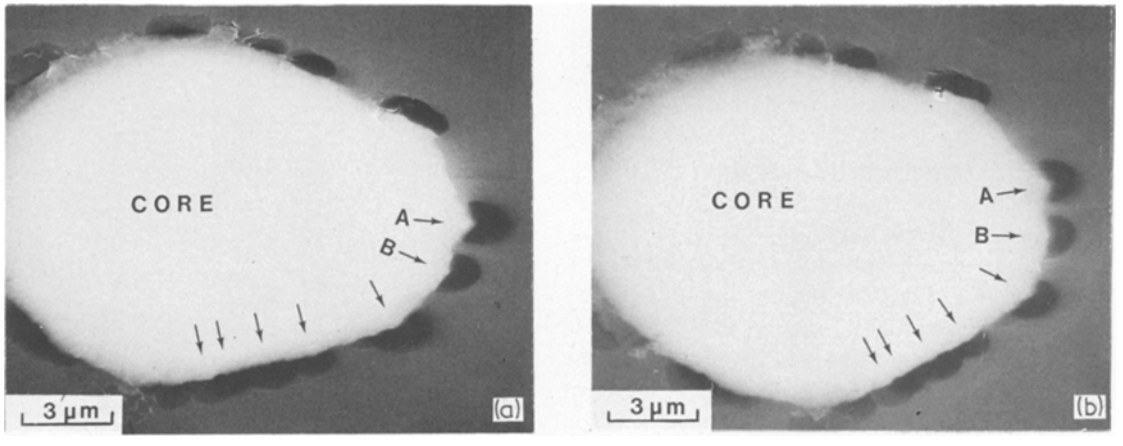

Figure 3 Successive cross-sections (<0.2 µm apart, due to 30 min additional ion etching) of boron fibre in the initial stages of mantle growth. The arrows mark nodule nucleation on die-mark ridges. (200 kV SEM)

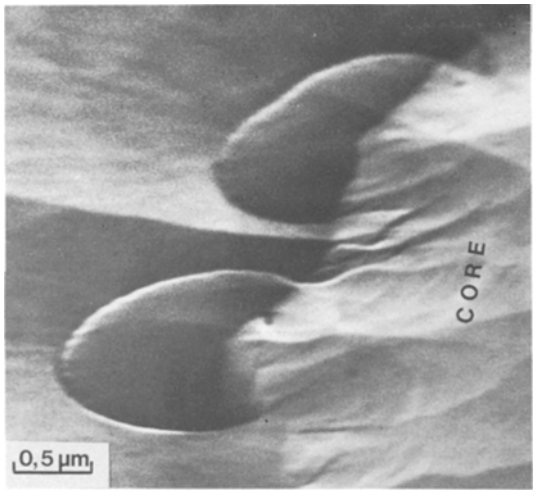

Figure 4 The boron nodules at A and B in Fig. 3, after 30 min ion etching. (200 kV SEM)

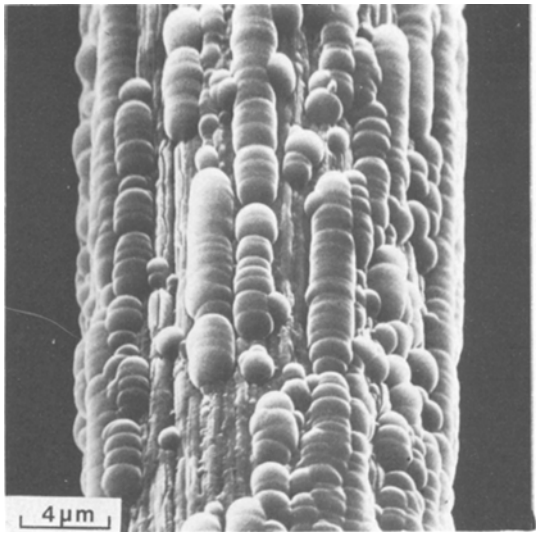

Figure 5 Axial rows of newly nucleated boron nodules. (20 kV SEM)

(Fig. 7). Simultaneously, boron is lost from the substrate surface by diffusion into the substrate under the formation of borides (Fig. 6a). The diffusion rate, which is initially equal to the deposition rate, later decreases with increasing boride layer thickness (Fig. 7). For geometrical reasons (see Fig. 6), it is obvious that the thickness of the boride layer increases at a higher rate under a ridge than under a groove. Consequently, the critical surface concentration for nucleation of a boron nodule is reached earlier on a ridge than in a groove (Fig. 6b).

(ii) It is well known that the increase in free surface energy of a growing surface layer depends on the radius of curvature of the substrate (and of the growing layer) in such a way that the layer would grow faster in thickness on concave than on convex substrate parts, i.e. faster in the bottom of a groove than at the tip of a ridge in the present case. This is the basis of the common observation that rough substrate surfaces are smoothed out by a depositing layer.

The present investigation proves experimentally that the high diffusivity of boron makes the on-ridge nodule nucleation according to mechanism (i) dominate over the in-groove nucleation according to (ii). Further, the observed tight distribution of nodules along the ridges is probably induced by closely spaced surface steps, so called scales [8], across the ridges, which are a typical result of adhesive contact and shear fracture between die and wire, during the wire drawing.

This observation is not contradictory to Wawner's observation of nucleation along scratches. His light optical images (Figs 10.6a and b of [1]) show either two nodule rows surrounded and separated by nucleation denuded zones, or one nodule row surrounded by denuded zones.

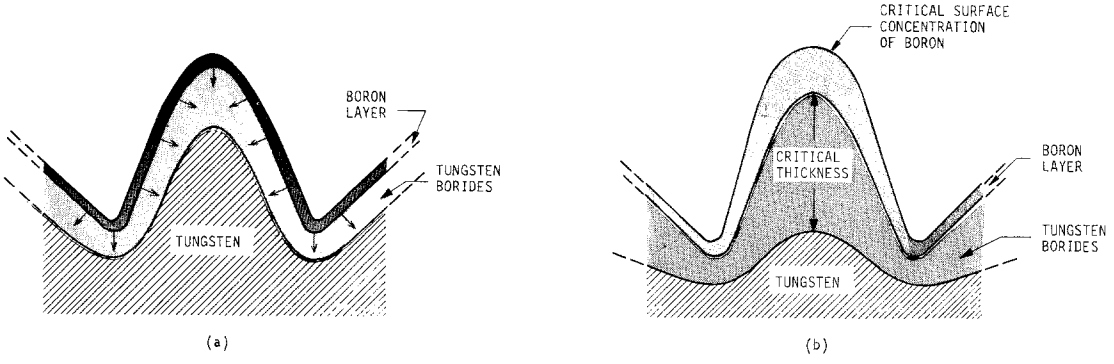

Figure 6(a) Initial deposition of a boron layer, and boron diffusion into the tungsten. (b) Relation between boron layer thickness and boride layer growth.

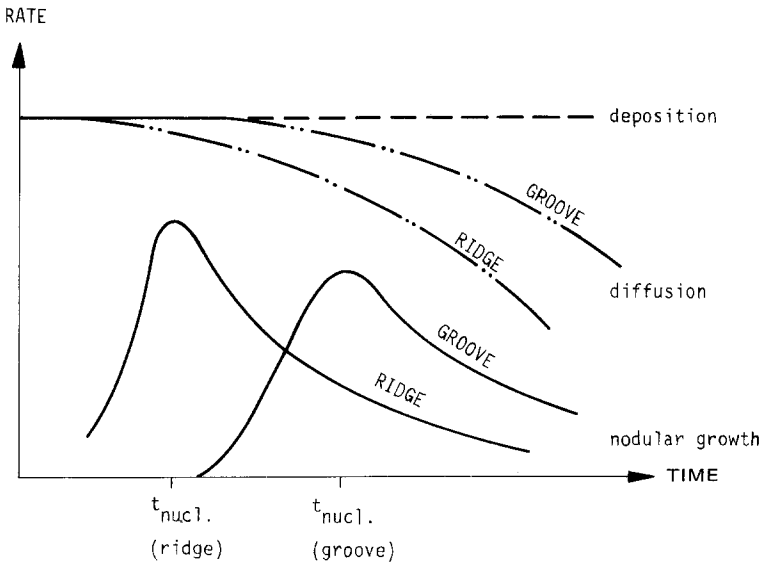

Figure 7 Rate-controlled nucleation of boron nodules. $t_{nucl.}$ corresponds to the attainment of the critical surface density of boron.

Although impossible to resolve in his images, this probably corresponds to the case of two ridges of displaced material on both sides of a normal scratch, or one ridge at one side of an oblique scratch.

3.2.2. Nodular growth

The general impression of SEM micrographs of the type of Fig. 5 is that the boron nodules grow with an obtuse contact angle on the substrate. The present technique of studying consecutive equally spaced normal planes, demonstrated in Fig. 3 provides a means of measuring the material characteristic contact angle θ. Fig. 8 shows cross-sections through nodules schematically with θ defined in an equatorial plane. The corresponding angle θ', observed in a SEM image of an arbitrary section, parallel to the equatorial plane, depends on the distance Δ between the plane of observation and the equatorial plane, as demonstrated by Fig. 8.

For the case of obtuse θ (Fig. 8a), θ' increases with Δ within the interval $\theta \leqslant \theta' \leqslant \pi$. θ' is, always obtuse, however. The semi-spherical geometry is simplified to $\theta = \theta' = \pi$ irrespective of Δ (Fig. 8b). Acute contact angles imply that θ' decreases with Δ within the interval (Fig. 8c) $0 \leqslant \theta' \leqslant \theta$. In this case, θ' is always acute. It is obvious from Fig. 8 that obtuse angles cannot be mistaken for acute angles or viceversa, and that θ is experimentally obtained as $\theta \lesssim \inf(\theta')$ for the obtuse case, and as $\theta \gtrsim \sup(\theta')$ for the acute case.

In the present investigation the contact angle is found to be obtuse. Measurements of θ' give the interval $100° \leqslant \theta' \leqslant 140°$ and thus an experimental value $\theta \lesssim 100°$.

3.2.3. Formation of proximate voids

Consider an axial row of boron nodules. Two adjacent growing nodules will meet in a point at a distance h above the substrate surface according to Fig. 9, and thereby hedge in a short channel of height h. Assuming an average nucleus spacing x, the equation

$$h = -\tfrac{1}{2}\, x \cos\theta \qquad (1)$$

gives the relation to the contact angle θ. During the successive nodule growth, the reactive gas mixture has full access to the whole free boron surface. Therefore, the channels will gradually be filled from the boron side, according to mechanism (ii) and from the core side by diffusional growth according to mechanism (i) in Section 3.2.1. The latter process implies a slight radial axpansion of the core under the formation of higher borides.

By this process, growing nodules combine in the axial dierction whereby rather smooth boron prisms will be formed, as observed in Fig. 10. During the continued growth, adjacent prisms will meet. The geometry is the same as that suggested in Fig. 9, with the nodule interdistance x replaced by the distance X between the axis of adjacent prisms. Again, contact will be established, but now

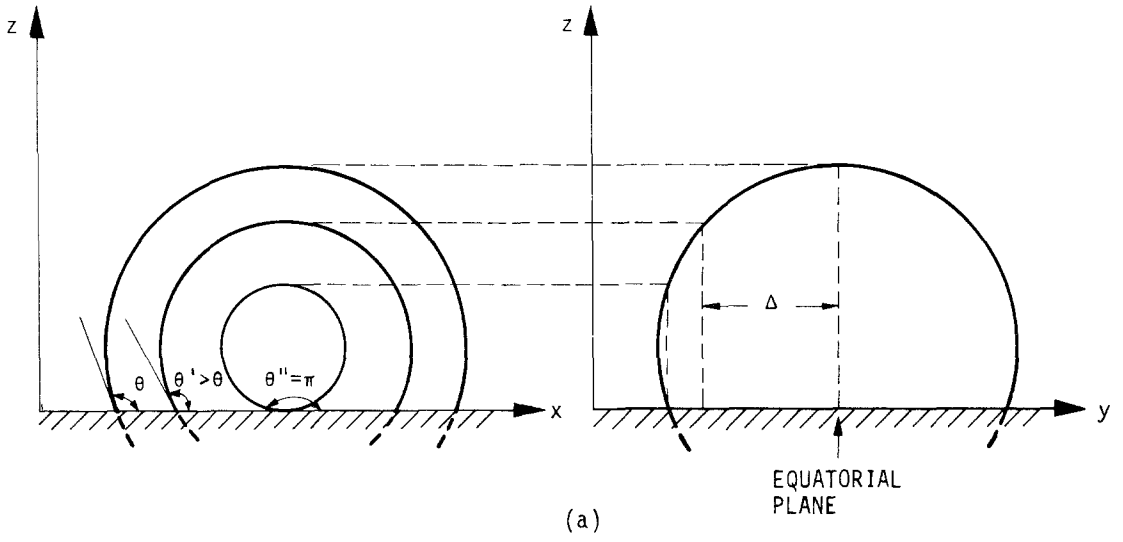

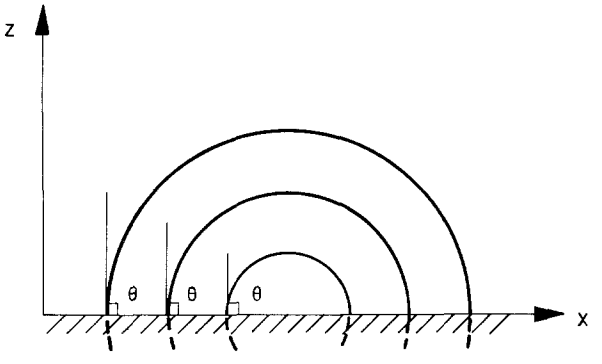

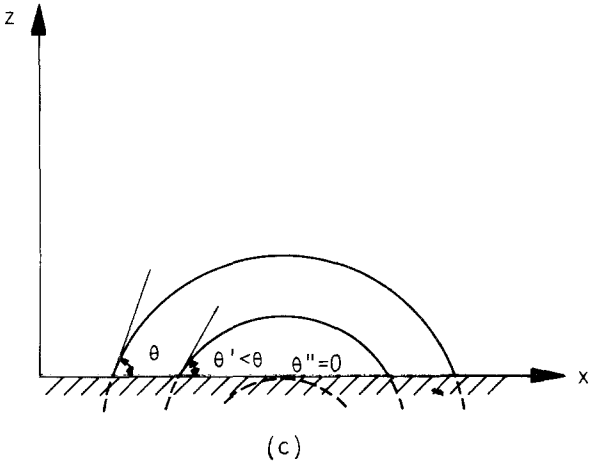

Figure 8 Schematic demonstration of the different cases of contact angle θ, and the effect of axial position of the plane of observation. (a) Obtuse (b) Normal (c) Acute.

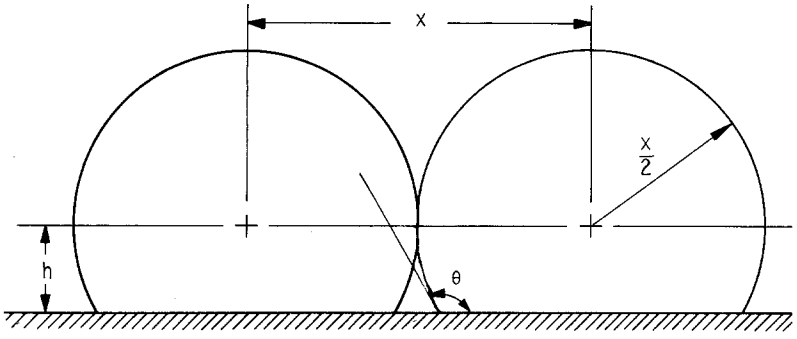

Figure 9 Surface contact between growing nodules of equal size. The contact (wetting) angle θ is obtuse

along a line at a distance H_0 above the nominal core surface. Equation 1 becomes

$$H_0 = -\tfrac{1}{2} X \cos\theta \qquad (2)$$

where X can be measured in SEM micrographs. A long axial void has now been hedged in, and is essentially protected from access of the reactants and thus from further deposition of boron. Subsequent core expansion may easily change the void morphology. A change in volume, however, requires self-diffusion over distances of the order of a nodule diameter, and involves transport of vacancies from one void to another.

The resulting morphology will be characterized by long axial voids just outside the core. In principle the radial extension is H_0, but the cross section has inherited the irregularity of the initial boron prism surfaces. The void will have a more or less sharp bulge, particularly when the axial position of one nodule boundary from each prism coincide. Continued diffusion is, however, expected to have a surface smoothing effect. A drawing of a void, formed by this mechanism, is reproduced in Fig. 11 (cf [4] Fig. 4).

All nodules are not necessarily nucleated simultaneously. Consequently, nodules of different size may interact by the same mechanisms as described for equal nodules. It is easily shown that the resulting voids decrease in height with increasing size difference.

Experimental X values from the present investigation are (in μm) $1 \leqslant X \leqslant 2$ which corresponds to $0.1 \leqslant H_0 \leqslant 0.2$.

Fig. 9 represents an idealized geometry, with a flat substrate surface. The additional influence of the real die-mark topography is indicated in Fig. 12. With the geometry of the figure the relation

$$H = \frac{X}{2}\{\tan v\,[1 - \sin(\theta + v)] - \cos(\theta + v)\} \qquad (3)$$

is obtained, and shows that the actual void height H increases with the "groove angle" v. Fig. 13 is a plot of Equation 3 for $\theta = 100°$. Normally, v is hardly expected to exceed some 20°, corresponding to a void height in the interval (in μm) $0.25 \leqslant H \leqslant 0.50$.

Fig. 14 is an example of a structure, interpreted as such a void. Dimensionally, this type of pore is far too small to be identified as the "proximate voids" described by Layden [2] and Vega and Vingsbo [3, 4]. Occasionally, however, groove angles of as much as 45° and even larger have been observed, which according to Equation 3 corres-

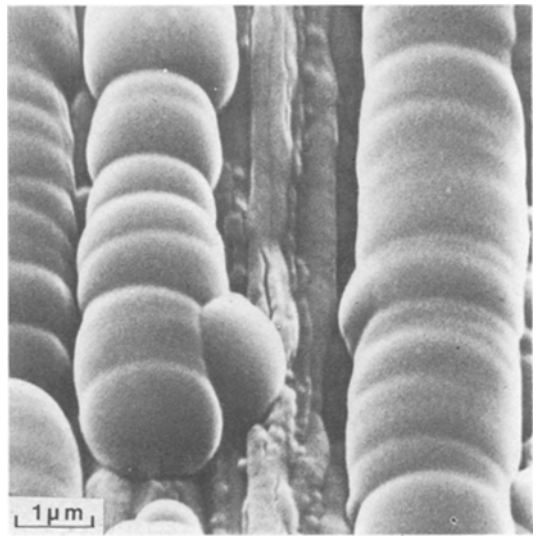

Figure 10 Axial row ("prism") of boron nodules. (20 kV SEM)

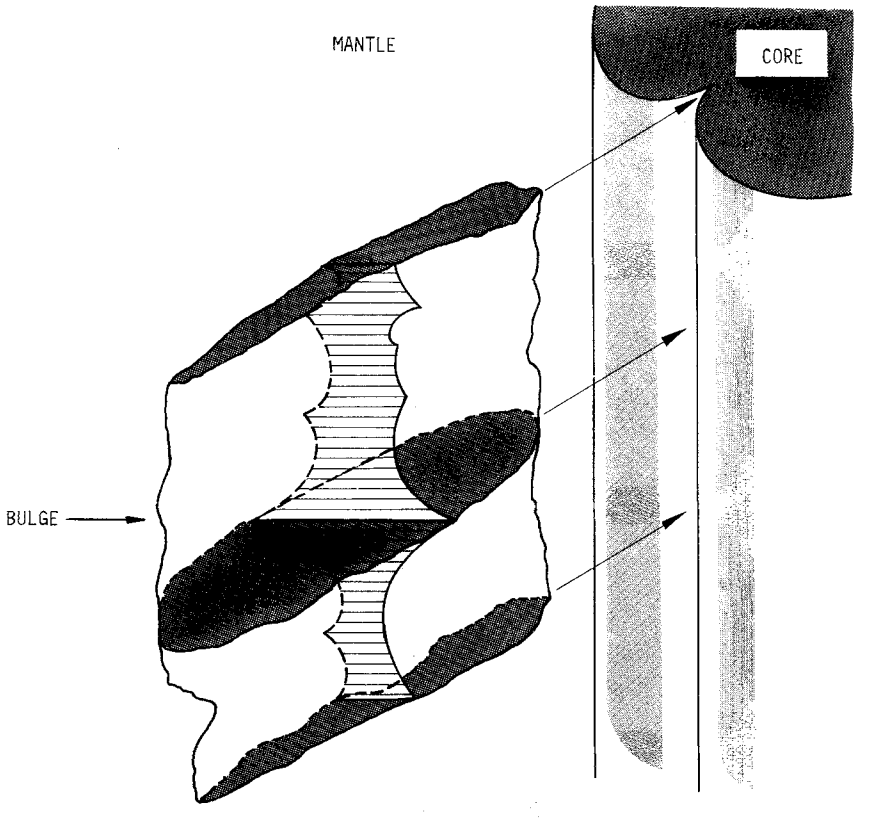

Figure 11 Schematic representation of proximate void.

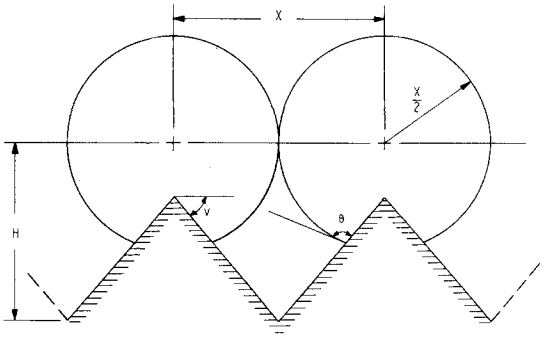

Figure 12 Surface contact between growing nodules of equal size, nucleated on neighbouring die-mark ridges of groove angle v.

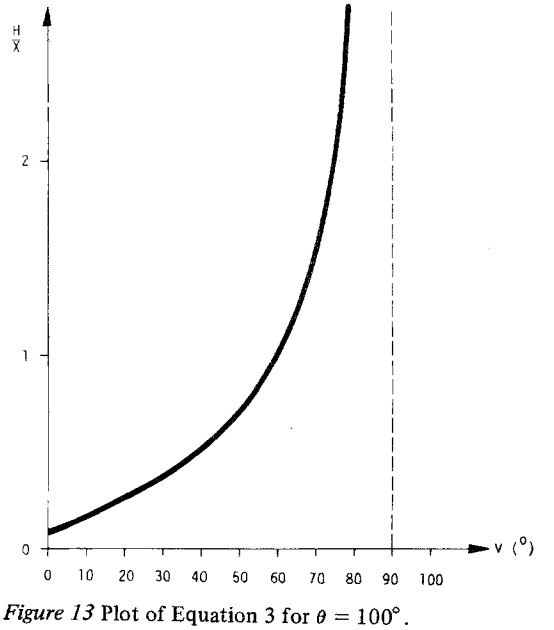

Figure 13 Plot of Equation 3 for $\theta = 100°$.

ponds to H values of the order of 1 μm. An image example of a void of this dimension is given in Fig. 15. Like all similar examples, it is situated immediately outside a deep groove, of considerably higher groove angle v than the average. The corresponding observed H values vary within the interval (μm) $1 < H < 3$.

From fractographic studies (see the fracture surface pair of Fig. 15), these voids are found to act as crack nuclei and are recognized as proximate voids. The formation mechanism suggested here explains the position, size and morphology, irregularities included, indicated by earler studies [4, 5].

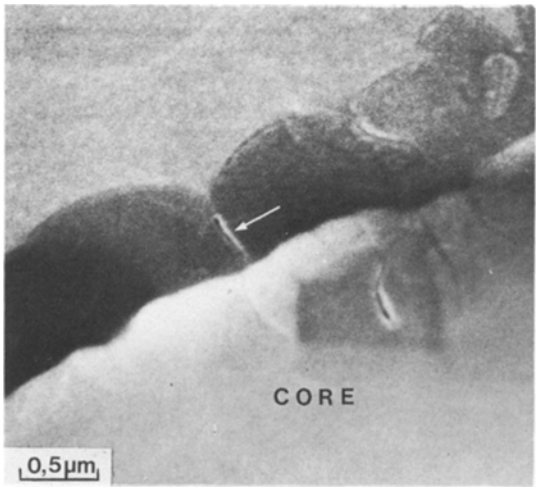

Figure 14 200 kV SEM micrograph of a polished section through a void (arrow) at a die-mark groove of low groove angle $v \sim 15°$ ($H \sim H_0 \sim 0.2\,\mu m$).

The cross-section of a proximate void may change considerably during the rapid diffusion processes, active at the high deposition temperature. The void can play an important role in the exchange of boron between mantle and core during the core growth [3]. This mechanism involves boron self-diffusion over distances of the order of $3\,\mu m$. The fact that proximate voids smaller than $1\,\mu m$ were rarely observed may thus be explained by coalescence, i.e. by vacancy diffusion from small voids, over distances of the order of X, to big voids. Measurements of the activation energy for self-diffusion [3] show that this process is possible under the experimental conditions prevailing during the deposition.

Acknowledgements

The tungsten wire was provided by LUMALAMPAN AB Stockholm and is hereby gratefully acknowledged.

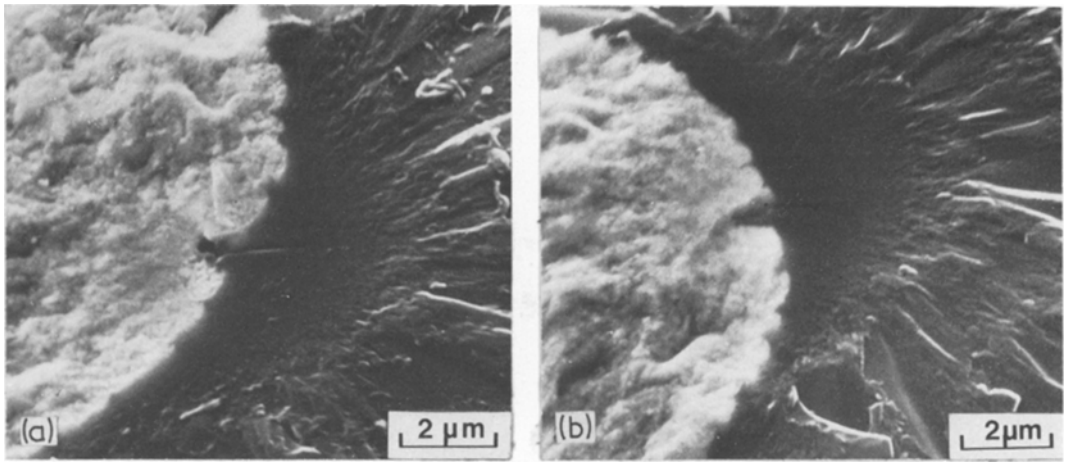

Figure 15 20 kV SEM micrograph of a fracture surface pair with a proximate void in a die-mark groove of high groove angle $v \sim 60°$ ($H \sim 2\,\mu m$. Fracture initiation can be traced to the void by extending the hackle marks through the mirror zone.

References

1. F. E. WAWNER JR., in "Modern Composite Materials", edited by L. J. Broutman and R. H. Krock (Addison Wesley, Reading USA, 1967).
2. G. K. LAYDEN, *J. Mater. Sci.* 8 (1973) 1581.
3. J. VEGA-BOGGIO and O. VINGSBO, *ibid* 11 (1976) 273.
4. *Idem, ibid* 11 (1976) 2242.
5. J. VEGA-BOGGIO, J.-Å. SCHWEITZ and O. VINGSBO, *ibid.* 12 (1977) 1692.
6. J. O. CARLSSON, to be published.
7. S. HOGMARK, H. SWAHN and O. VINGSBO, *Ultramicroscopy* 1 (1975) 113.
8. S. HOGMARK and O. VINGSBO, *Wear* 31 (1975) 39.

Received 13 December 1976 and accepted 8 February 1977.